

IMPERIAL COLLEGE LONDON

DEPARTMENT OF ELECTRICAL AND ELECTRONIC ENGINEERING  
EXAMINATIONS 2009

MSc and EEE PART IV: MEng and ACGI

**RADIO FREQUENCY ELECTRONICS**

Corrected Copy

Monday, 11 May 10:00 am

Time allowed: 3:00 hours

**There are SIX questions on this paper.**

**Answer FOUR questions.**

*All questions carry equal marks*

**Any special instructions for invigilators and information for candidates are on page 1.**

Examiners responsible	First Marker(s) :	S. Lucyszyn
	Second Marker(s) :	E. Rodriguez-Villegas

**Special instructions for invigilators:** This is a Closed Book examination.  
A Smith Chart is to be distributed.

**Information for candidates:** This is a Closed Book examination.  
Filter curves and filter tables are attached at the back.  
A Smith Chart is provided and, if used, you must attach this  
to your answer book.

## The Questions

1.

- a) The frequency spectrum has limits on performance and low cost exploitation.
- i) As frequency decreases below 1 GHz, what affects the signal/noise ratio of a wireless communications system? [2]
  - ii) Why is the frequency spectrum between 1 GHz and 10 GHz so convenient for commercial exploitation? [2]
  - iii) Where in the frequency spectrum are the water and oxygen absorption peaks, between 10 GHz and 200 GHz? [2]
  - iv) What is significant about the 38 GHz and 94 GHz frequency bands? Give an appropriate application for each band and state the reasons for choosing these applications. [2]
  - v) What is significant about the 60 GHz frequency band? Give two applications for this band and state the reasons for choosing these applications. [2]
- b) Compare and contrast hybrid and monolithic technologies for realising microwave integrated circuits. [5]
- c) Draw the block diagram for a TVRO LNB. For each block, comment on the suitability for their implementation using monolithic technology. [5]

2. A transistor has an input impedance of  $+10 - j10 \, \Omega$  at 1.9 GHz. This transistor must be impedance matched to a signal generator having a  $50 \, \Omega$  source impedance. Four-element matching networks are required, such that the first three sequential points on an impedance Smith chart are  $(+10 - j10 \, \Omega)$ ,  $(+10 + j10 \, \Omega)$  and  $(+20 + j0 \, \Omega)$ .
- (a) With the aid of a Smith chart, design the matching network using only lossless, air-filled, coaxial transmission lines having a characteristic impedance of  $50 \, \Omega$ . You must draw the topology of the matching network, indicating the role of each element, and give the physical lengths of all the transmission lines. [7]
- (b) What are the unloaded quality factors at each of the five points on the Smith chart with the design in 2(a)? [2]
- (c) With the aid of a Smith chart, design the matching network using only lossless lumped-element components. You must draw the topology of the matching network, indicating the value for each of the components. [7]
- (d) What are the unloaded quality factors at each of the five points on the Smith chart with the design in 2(c)? [2]
- (e) How does the worst-case value of unloaded quality factor in 2(d) compare with that in 2(b) and what is the significance of this in terms of the operational bandwidth of the matching network?. [2]

3.

- (a) Given a square wave signal generator, with a clock frequency that can vary between zero and 1000 MHz, propose how this could be used to generate a sinusoidal signal at a frequency of 1800 MHz.

[4]

- (b) Design a lumped-element  $L$ - $C$  high-pass filter to meet the following specifications:

Pass band attenuation ripple	0.1 dB
-3 dB cut-off frequency:	1500 MHz
Stop band frequency:	600 MHz
Stop band attenuation:	> 70 dB
Source impedance, $Z_s$ :	50 $\Omega$
Load impedance, $Z_L$ :	50 $\Omega$

[10]

- (c) Determine the worst-case levels of return losses within both the pass band and the stop band for the filter in 3(b). How could the stop band return loss adversely effect the implementation of 3(a) and suggest a suitable topology for overcoming this problem?

[6]

4.

- (a) Explain the advantages of using  $S$ -parameters over other types of parameters and comment on which parameters commercial RF circuit simulators use to perform their analysis.  
[5]
- (b) Using appropriate diagrams describe the use of stability circles and indicate all the various conditions of stability. How do these conditions relate to Rollett's stability factor?  
[5]
- (c) In terms of power ratios, define *Insertion Power Gain*, *Forward Transducer Power Gain*, *Operating Power Gain* and *Available Power Gain*. Briefly explain the applications of each definition.  
[5]
- (d) Given a transistor with small-signal  $S$ -parameters of  $S_{21} = 6.5 - j 3.7$  and  $S_{12} = 0.2 + j 0.1$  and also a Rollett's stability factor,  $K = 1.27$ , calculate the Maximum Stable Gain and Maximum Available Gain. What are the roll-off frequency characteristics for these gains?  
[5]

5.

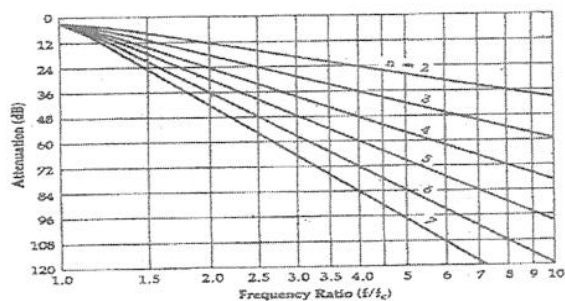
- (a) With the aid of a diagram and simple S-parameter analysis, explain how a lossless single-stage reflection-topology works. [7]
- (b) Explain how an ideal reflection-type attenuator can be implemented and extend the analysis given in 5(a) for this application. [5]
- (c) Explain how an ideal reflection-type phase shifter can be implemented and extend the analysis given in 5(a) for this application. [5]
- (d) Describe the inherent drawbacks of the applications given in 5(b) and 5(c) at microwave frequencies when non-ideal components are used. How can a useful vector modulator be implemented with non-ideal components. [3]

6.

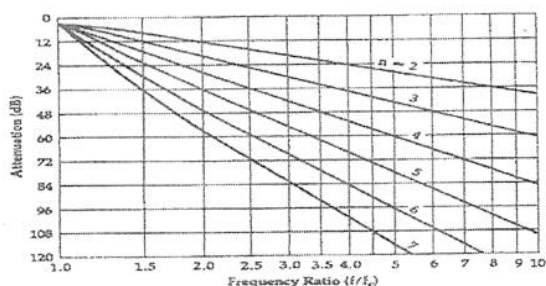
- (a) Describe a scalar network analyser and draw the simplified block diagram for a vector network analyser (VNA), clearly identifying all blocks. Explain how transmission measurements are performed with the VNA and list some of the advantages and disadvantages of both instruments. [8]
- (b) Compare and contrast test-fixture measurements with on-wafer probing. [4]
- (c) Briefly explain the basic principles by which a VNA can perform synthetic-pulse time domain reflectometry. Sketch the measured reflection response in the time domain for a slightly mismatched MMIC through-line embedded within a non-ideal test fixture. Describe how the frequency response of  $|S_{11}|$  can be emphasised for the embedded MMIC. Is this 'de-embedding' process needed with on-wafer probing? [8]



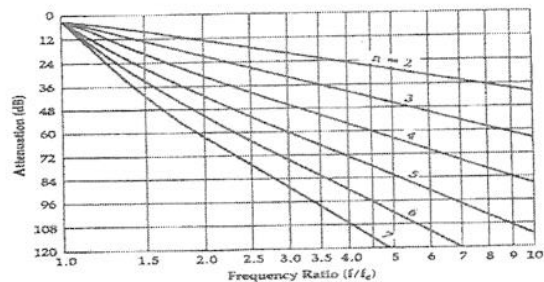
## Filter tables



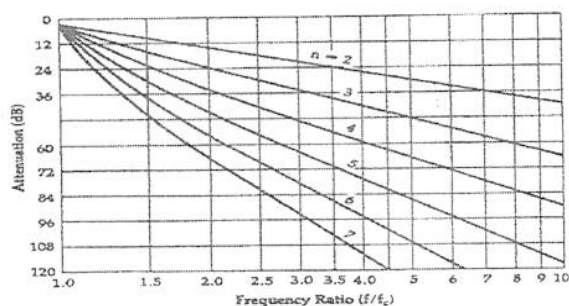
Attenuation characteristics for Butterworth filters.



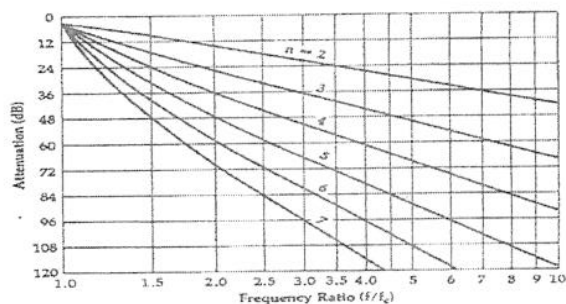
Attenuation characteristics for a Chebyshev filter with 0.01-dB ripple.



Attenuation characteristics for a Chebyshev filter with 0.1-dB ripple.

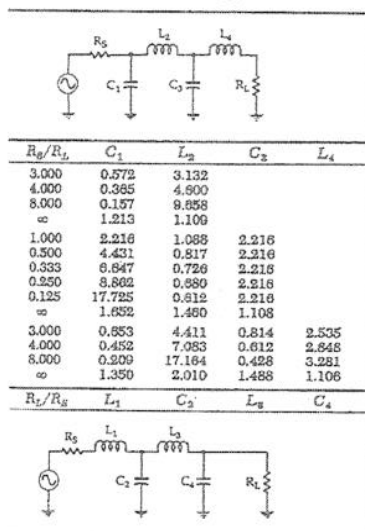


Attenuation characteristics for a Chebyshev filter with 0.5-dB ripple.

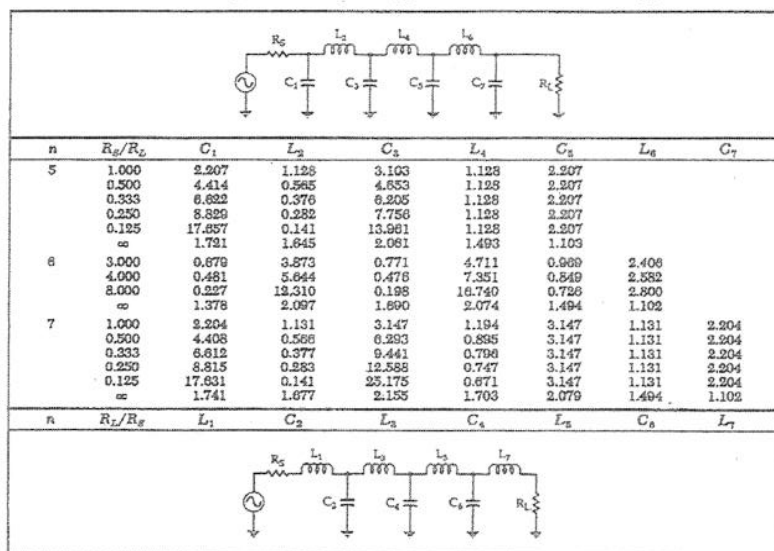


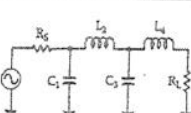
Attenuation characteristics for a Chebyshev filter with 1-dB ripple.

Chebyshev Low-Pass Prototype Element Values for 1.0-dB Ripple

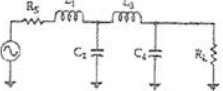
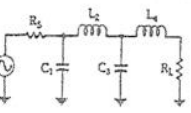


Chebyshev Low-Pass Prototype Element Values for 1.0-dB Ripple

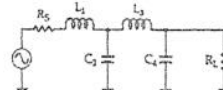


Butterworth Low-Pass  
Prototype Element Values


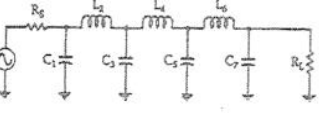
$n$	$R_g/R_L$	$C_1$	$L_2$	$C_2$	$L_3$
2	1.111	1.035	1.835		
	1.250	0.849	2.121		
	1.429	0.697	2.439		
	1.667	0.586	2.828		
	2.000	0.448	3.346		
	2.500	0.342	4.095		
	3.333	0.245	5.313		
	5.000	0.156	7.707		
	10.000	0.074	14.814		
$\infty$	1.414	0.707			
3	0.900	0.808	1.633	1.599	
	0.800	0.844	1.394	1.928	
	0.700	0.915	1.185	2.277	
	0.600	1.023	0.965	2.702	
	0.500	1.181	0.779	3.261	
	0.400	1.425	0.604	4.064	
	0.300	1.838	0.440	5.363	
	0.200	2.669	0.284	7.910	
	0.100	5.187	0.138	15.455	
$\infty$	1.500	1.333	0.500		
4	1.111	0.468	1.592	1.744	1.489
	1.250	0.388	1.695	1.511	1.811
	1.429	0.325	1.862	1.291	2.175
	1.667	0.269	2.103	1.082	2.613
	2.000	0.218	2.452	0.883	3.187
	2.500	0.169	2.986	0.691	4.009
	3.333	0.124	3.883	0.507	5.338
	5.000	0.080	5.894	0.331	7.940
	10.000	0.038	11.094	0.182	15.642
$\infty$	1.531	1.577	1.082	0.383	


Chebyshev Low-Pass Element Values  
for 0.01-dB Ripple


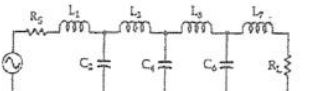
$n$	$R_g/R_L$	$C_1$	$L_2$	$C_2$	$L_3$
2	1.101	1.347	1.483		
	1.111	1.247	1.592		
	1.250	0.943	1.997		
	1.429	0.750	2.344		
	1.667	0.609	2.750		
	2.000	0.479	3.277		
	2.500	0.363	4.033		
	3.333	0.259	5.255		
	5.000	0.164	7.650		
	10.000	0.078	14.749		
$\infty$	1.418	0.742			
3	1.000	1.181	1.821	1.181	
	0.900	1.092	1.660	1.480	
	0.800	1.097	1.443	1.806	
	0.700	1.160	1.228	2.165	
	0.600	1.274	1.024	2.588	
	0.500	1.452	0.829	3.164	
	0.400	1.734	0.645	3.974	
	0.300	2.218	0.470	5.280	
	0.200	3.193	0.305	7.834	
	0.100	8.141	0.148	15.390	
$\infty$	1.501	1.433	0.591		
4	1.100	0.850	1.838	1.761	1.046
	1.111	0.854	1.946	1.744	1.165
	1.250	0.618	2.075	1.542	1.617
	1.429	0.495	2.279	1.334	2.008
	1.667	0.398	2.571	1.128	2.461
	2.000	0.316	2.994	0.926	3.045
	2.500	0.242	3.641	0.726	3.875
	3.333	0.174	4.727	0.538	5.209
	5.000	0.112	6.910	0.352	7.813
	10.000	0.054	13.469	0.173	15.510
$\infty$	1.529	1.694	1.312	0.523	



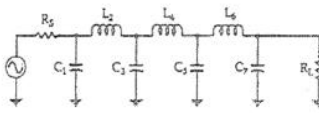
Butterworth Low-Pass Prototype Element Values



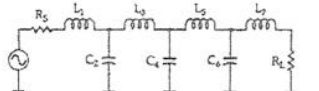
$n$	$R_g/R_L$	$C_1$	$L_2$	$C_3$	$L_4$	$C_5$	$L_6$	$C_7$
5	0.900	0.442	1.027	1.910	1.756	1.399		
	0.800	0.470	0.866	2.081	1.544	1.738		
	0.700	0.517	0.731	2.285	1.333	2.108		
	0.600	0.586	0.609	2.600	1.126	2.552		
	0.500	0.686	0.496	3.051	0.924	3.133		
	0.400	0.838	0.388	3.736	0.727	3.985		
	0.300	1.094	0.285	4.884	0.537	5.307		
	0.200	1.608	0.188	7.185	0.352	7.935		
	0.100	3.512	0.091	14.095	0.173	15.710		
$\infty$	1.545	1.694	1.382	0.894		0.309		
6	1.111	0.269	1.040	1.322	2.054	1.744	1.335	
	1.250	0.245	1.116	1.126	2.239	1.550	1.688	
	1.429	0.207	1.236	0.957	2.499	1.346	2.082	
	1.667	0.173	1.407	0.801	2.858	1.143	2.509	
	2.000	0.141	1.653	0.654	3.309	0.942	3.094	
	2.500	0.111	2.028	0.514	4.141	0.745	3.931	
	3.333	0.082	2.656	0.379	5.433	0.552	5.290	
	5.000	0.054	3.917	0.248	8.020	0.343	7.922	
	10.000	0.026	7.705	0.122	15.788	0.179	15.738	
$\infty$	1.553	1.759	1.553	1.202	0.758	0.259		
7	0.900	0.299	0.711	1.404	1.489	2.125	1.727	1.296
	0.800	0.322	0.606	1.517	1.278	2.334	1.546	1.652
	0.700	0.357	0.515	1.688	1.091	2.618	1.350	2.028
	0.600	0.408	0.432	1.928	0.917	3.005	1.150	2.477
	0.500	0.480	0.354	2.273	0.751	3.553	0.951	3.064
	0.400	0.590	0.278	2.795	0.592	4.360	0.754	3.904
	0.300	0.775	0.206	3.671	0.437	5.761	0.560	5.258
	0.200	1.145	0.135	5.427	0.287	8.526	0.369	7.908
	0.100	2.257	0.067	10.700	0.142	16.822	0.182	15.748
$\infty$	1.558	1.799	1.659	1.397	1.055	0.658	0.223	



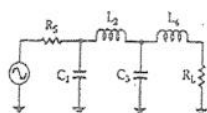
Chebyshev Low-Pass Element Values for 0.01-dB Ripple



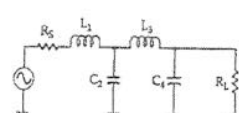
$n$	$R_g/R_L$	$C_1$	$L_2$	$C_3$	$L_4$	$C_5$	$L_6$	$C_7$
5	1.000	0.977	1.685	2.037	1.685	0.977		
	0.900	0.880	1.456	2.174	1.641	1.274		
	0.800	0.877	1.235	2.376	1.499	1.607		
	0.700	0.926	1.040	2.658	1.323	1.977		
	0.600	1.019	0.863	3.041	1.135	2.424		
	0.500	1.166	0.699	3.584	0.942	3.009		
	0.400	1.398	0.544	4.403	0.749	3.845		
	0.300	1.797	0.398	5.779	0.557	5.193		
	0.200	2.604	0.259	8.514	0.368	7.828		
	0.100	5.041	0.127	16.741	0.182	15.613		
$\infty$	1.547	1.795	1.645	1.237	0.488			
6	1.101	0.851	1.796	1.841	2.027	1.631	0.937	
	1.111	0.760	1.732	1.775	2.094	1.638	1.053	
	1.250	0.545	1.854	1.489	2.403	1.507	1.504	
	1.429	0.436	2.038	1.268	2.735	1.332	1.899	
	1.667	0.351	2.298	1.061	3.167	1.145	2.357	
	2.000	0.279	2.676	0.867	3.766	0.954	2.948	
	2.500	0.214	3.261	0.682	4.667	0.761	3.790	
	3.333	0.155	4.245	0.503	6.163	0.568	5.143	
	5.000	0.100	6.323	0.330	9.151	0.376	7.785	
	10.000	0.048	12.171	0.162	18.105	0.187	15.595	
$\infty$	1.551	1.847	1.790	1.598	1.190	0.468		
7	1.000	0.913	1.595	2.002	1.870	2.002	1.555	0.913
	0.900	0.818	1.382	2.080	1.722	2.202	1.581	1.206
	0.800	0.811	1.150	2.202	1.525	2.465	1.464	1.538
	0.700	0.857	0.967	2.516	1.323	2.802	1.307	1.910
	0.600	0.943	0.803	2.872	1.124	3.250	1.131	2.359
	0.500	1.080	0.650	3.382	0.928	3.875	0.947	2.948
	0.400	1.297	0.507	4.156	0.735	4.812	0.758	3.790
	0.300	1.699	0.372	5.454	0.540	6.370	0.568	5.148
	0.200	2.242	0.242	6.057	0.360	9.484	0.378	7.802
	0.100	4.701	0.119	15.872	0.178	18.818	0.188	15.652
$\infty$	1.559	1.867	1.866	1.765	1.563	1.161	0.456	



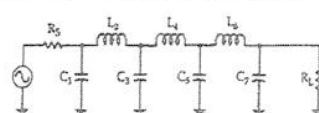
Chebyshev Low-Pass Prototype Element Values for 0.1-dB Ripple



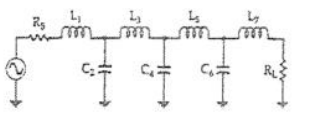
n	$R_g/R_L$	$C_1$	$L_2$	$C_3$	$L_4$
2	1.355	1.209	1.638		
	1.429	0.977	1.982		
	1.687	0.733	2.468		
	2.000	0.580	3.054		
	2.500	0.417	3.827		
	3.333	0.293	5.050		
	5.000	0.184	7.426		
	10.000	0.087	14.433		
	$\infty$	1.391	0.819		
3	1.000	1.433	1.594	1.433	
	0.900	1.426	1.494	1.622	
	0.800	1.451	1.356	1.871	
	0.700	1.521	1.183	2.190	
	0.600	1.648	1.017	2.603	
	0.500	1.853	0.838	3.159	
	0.400	2.186	0.660	3.908	
	0.300	2.763	0.488	5.279	
	0.200	3.942	0.317	7.850	
	0.100	7.512	0.155	15.466	
	$\infty$	1.513	1.510	0.716	
4	1.355	0.992	2.148	1.585	1.341
	1.429	0.779	2.348	1.429	1.700
	1.687	0.576	2.730	1.185	2.943
	2.000	0.440	3.227	0.967	2.858
	2.500	0.329	3.961	0.760	3.898
	3.333	0.233	5.178	0.590	5.030
	5.000	0.148	7.807	0.367	7.614
	10.000	0.070	14.887	0.180	15.230
	$\infty$	1.511	1.768	1.455	0.673



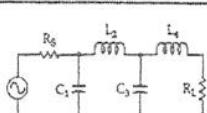
Chebyshev Low-Pass Prototype Element Values for 0.1-dB Ripple



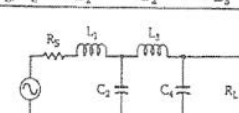
n	$R_g/R_L$	$C_1$	$L_2$	$C_3$	$L_4$	$C_5$	$L_6$	$C_7$
5	1.000	1.301	1.556	2.241	1.556	1.301		
	0.900	1.285	1.433	2.380	1.488	1.488		
	0.800	1.300	1.288	2.582	1.382	1.738		
	0.700	1.358	1.117	2.888	1.244	2.062		
	0.600	1.470	0.947	3.289	1.085	2.484		
	0.500	1.654	0.778	3.845	0.913	3.055		
	0.400	1.954	0.612	4.720	0.733	3.686		
	0.300	2.477	0.451	6.196	0.550	5.237		
	0.200	3.546	0.285	9.127	0.366	7.889		
	0.100	6.787	0.115	17.957	0.182	15.745		
	$\infty$	1.561	1.807	1.766	1.417	0.651		
6	1.355	0.942	2.080	1.659	2.247	1.534	1.277	
	1.429	0.735	2.249	1.454	2.544	1.405	1.628	
	1.687	0.542	2.600	1.183	3.064	1.185	2.174	
	2.000	0.414	3.068	0.958	3.712	0.979	2.794	
	2.500	0.310	3.765	0.749	4.651	0.778	3.645	
	3.333	0.230	4.927	0.551	6.195	0.580	4.996	
	5.000	0.139	7.250	0.361	9.261	0.384	7.618	
	10.000	0.067	14.220	0.178	18.427	0.190	15.350	
	$\infty$	1.534	1.884	1.831	1.749	1.394	0.638	
7	1.000	1.262	1.520	2.239	1.680	2.239	1.520	1.262
	0.900	1.242	1.395	2.361	1.578	2.367	1.459	1.447
	0.800	1.255	1.245	2.548	1.443	2.624	1.362	1.667
	0.700	1.310	1.083	2.819	1.283	2.942	1.233	2.021
	0.600	1.417	0.917	3.205	1.209	3.364	1.081	2.444
	0.500	1.585	0.753	3.764	0.928	4.015	0.914	3.018
	0.400	1.885	0.593	4.618	0.742	4.970	0.738	3.855
	0.300	2.392	0.437	6.054	0.556	6.569	0.557	5.217
	0.200	3.428	0.286	8.937	0.369	9.770	0.372	7.890
	0.100	6.570	0.141	17.603	0.184	19.376	0.186	15.813
	$\infty$	1.575	1.858	1.921	1.827	1.734	1.379	0.631



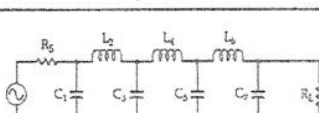
Chebyshev Low-Pass Prototype Element Values for 0.5-dB Ripple



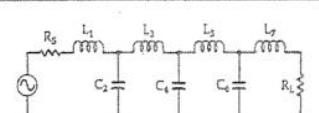
n	$R_g/R_L$	$C_1$	$L_2$	$C_3$	$L_4$
2	1.984	0.933	1.050		
	2.000	0.939	2.103		
	2.500	0.564	3.185		
	3.333	0.375	4.411		
	5.000	0.228	6.700		
	10.000	0.105	13.322		
	$\infty$	1.307	0.975		
3	1.000	1.864	1.280	1.834	
	0.900	1.918	1.209	2.026	
	0.800	1.997	1.120	2.237	
	0.700	2.114	1.015	2.517	
	0.500	2.557	0.759	3.436	
	0.400	2.985	0.615	4.242	
	0.300	3.729	0.463	5.576	
	0.200	5.254	0.309	8.225	
	0.100	9.890	0.153	18.118	
	$\infty$	1.572	1.518	0.932	
4	1.984	0.820	2.586	1.304	1.826
	2.000	0.845	2.720	1.238	1.965
	2.500	0.516	3.768	0.889	3.121
	3.333	0.344	5.120	0.621	4.450
	5.000	0.210	7.708	0.400	6.987
	10.000	0.098	15.352	0.194	14.262
	$\infty$	1.436	1.889	1.521	0.913



Chebyshev Low-Pass Prototype Element Values for 0.5-dB Ripple



n	$R_g/R_L$	$C_1$	$L_2$	$C_3$	$L_4$	$C_5$	$L_6$	$C_7$
5	1.000	1.807	1.303	2.691	1.303	1.807		
	0.900	1.854	1.222	2.849	1.238	1.970		
	0.800	1.926	1.126	3.060	1.157	2.185		
	0.700	2.035	1.015	3.353	1.058	2.470		
	0.600	2.200	0.890	3.765	0.942	2.861		
	0.500	2.457	0.754	4.367	0.810	3.414		
	0.400	2.870	0.609	5.296	0.664	4.245		
	0.300	3.588	0.459	6.871	0.506	5.625		
	0.200	5.064	0.306	10.054	0.343	8.397		
	0.100	9.558	0.153	19.647	0.173	16.574		
	$\infty$	1.830	1.740	1.922	1.514	0.903		
6	1.984	0.905	2.577	1.368	2.713	1.299	1.795	
	2.000	0.930	2.704	1.291	2.872	1.237	1.956	
	2.500	0.506	3.722	0.890	4.109	0.881	3.103	
	3.333	0.337	5.055	0.632	5.699	0.635	4.481	
	5.000	0.206	7.615	0.408	8.732	0.412	7.031	
	10.000	0.098	15.186	0.197	17.681	0.202	14.433	
7	1.000	1.790	1.296	2.718	1.385	2.718	1.296	1.790
	0.900	1.835	1.215	2.869	1.308	2.883	1.234	1.953
	0.800	1.905	1.118	3.076	1.215	3.107	1.155	2.188
	0.700	2.011	1.007	3.364	1.105	3.416	1.058	2.455
	0.600	2.174	0.882	3.772	0.979	3.852	0.944	2.846
	0.500	2.428	0.747	4.370	0.838	4.289	0.814	3.405
	0.400	2.835	0.604	5.295	0.685	5.470	0.666	4.243
	0.300	3.546	0.455	6.867	0.522	7.134	0.513	5.635
	0.200	5.007	0.303	10.049	0.352	10.496	0.348	8.404
	0.100	9.458	0.151	19.649	0.178	20.631	0.178	16.665
	$\infty$	1.646	1.777	2.031	1.789	1.924	1.503	0.885



Model answer to Q 1(a): Bookwork and Discussions in Class

- i) Signal/noise ratio becomes more problematic as frequency decreases below 1 GHz, because of the increase in galactic noise. As a result, more signal power is required to maintain a good signal/noise ratio. [2]
- ii) The frequency between 1 GHz and 10 GHz is convenient for commercial exploitation because both galactic and atmospheric noise are very low. Also, cheap lumped-element passive components and high gain active components can be used in this frequency band. [2]
- iii) The water absorption peaks are found at 22 GHz and 183 GHz; while the oxygen absorption peaks are found at 60 GHz and 119 GHz. [2]
- iv) At 38 GHz and 94 GHz there are troughs in the atmospheric attenuation curves. As a result, Line-of-Sight communication links (having wide bandwidths) and directional radar systems (having highly directional antennas) are used in these bands, respectively. [2]
- v) The 60 GHz band has very high atmospheric attenuation. As a result, it is ideal for indoor wireless local area network applications and inter-satellite communication links. The potential interference to other nearby services operating in the same band can be minimized by the inherent drop in signal strength, as distance increases. [2]

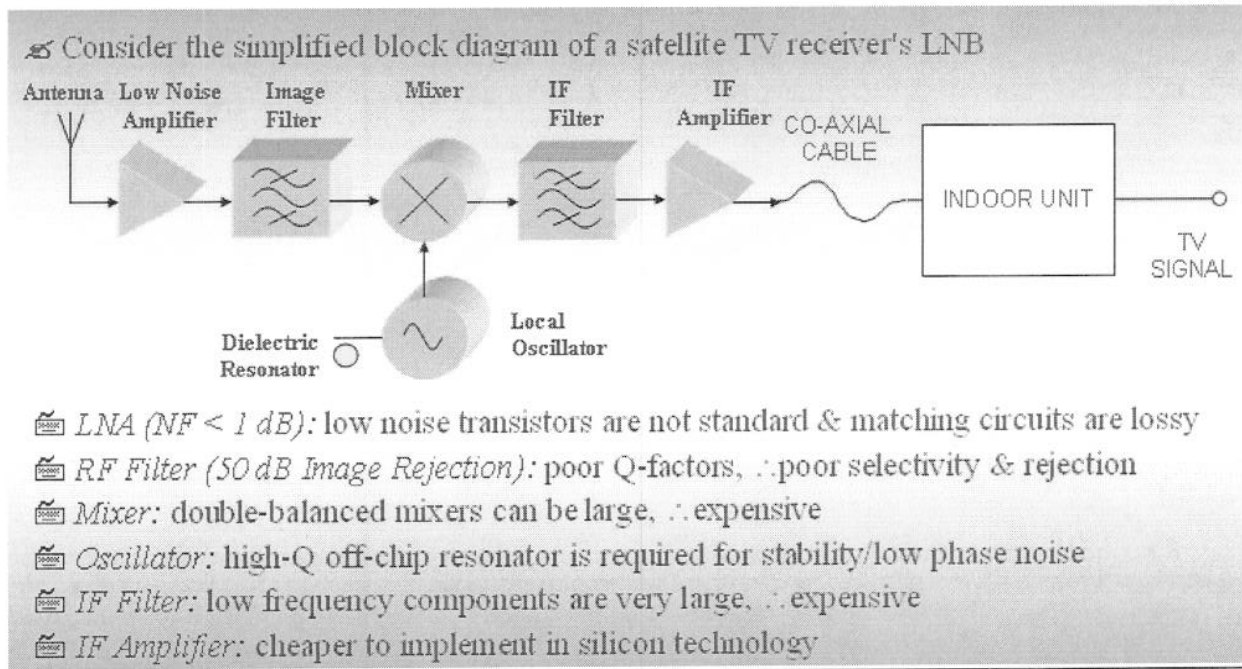
Model answer to Q 1(b): Bookwork

The Advantages/disadvantages of MMICs when compared with hybrid MICs are given in the Table below.

<i>MMICs</i>	<i>Hybrid MICs</i>
Cheap in large quantities; especially economical with many transistors	Large passive circuits can be cheaper; automatic assembly is possible
Very good reproducibility	Poor reproducibility due to device placement errors and bond-wires
Small and light	Compact multilayer substrates with embedded passives now available
Reliable	Hybrids are mostly 'glued' together and so reliability suffers
Less parasitics – more bandwidth and higher frequencies	Poor interconnects can kill the performance of individual components
Space is at a premium; the circuit must be made as small as possible	Substrate is cheap, which allows microstrip to be used abundantly
Very limited choice of component	A vast selection of passive components is available and the best transistors are always available for LNAs and PAs
Long turn around time (3 months)	Can be very fast (1 week), making multiple iterations possible
Very expensive to start up	Very little capital equipment is required

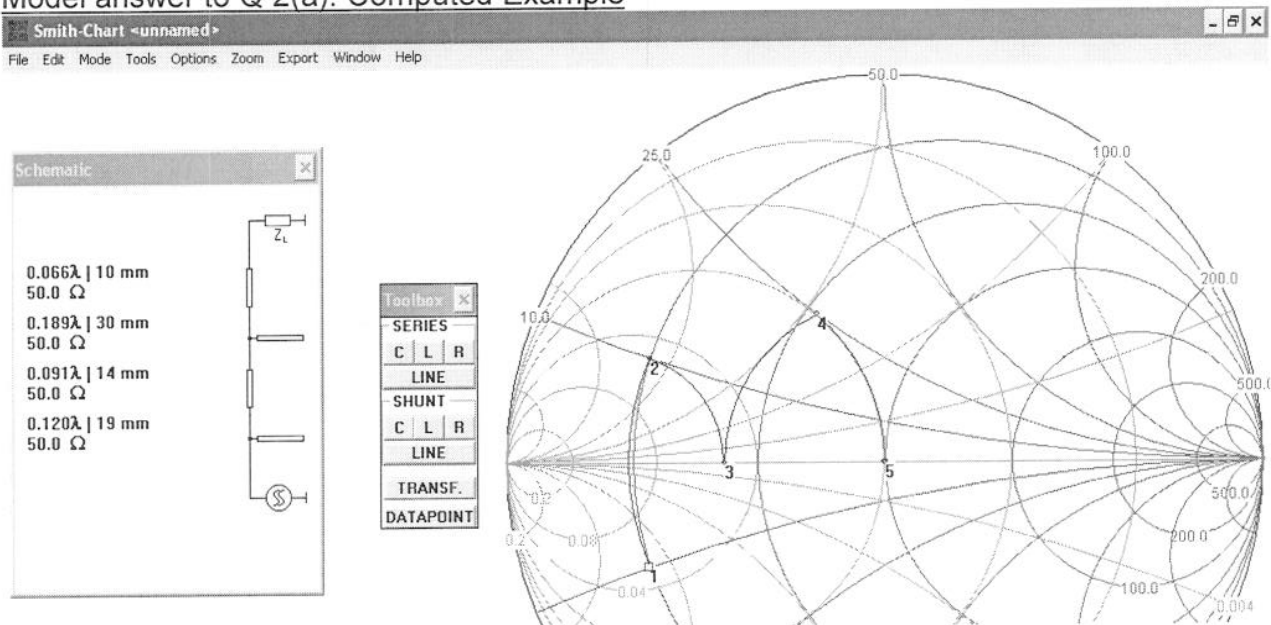
[5]

## Model answer to Q 1(c): Bookwork



[5]

## Model answer to Q 2(a): Computed Example

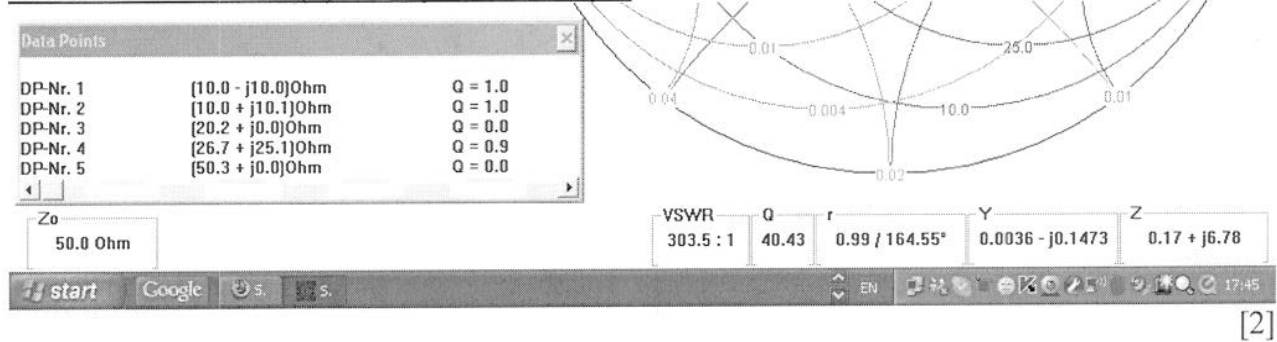


It can be seen that the open-circuit stubs act as synthesized shunt capacitances.

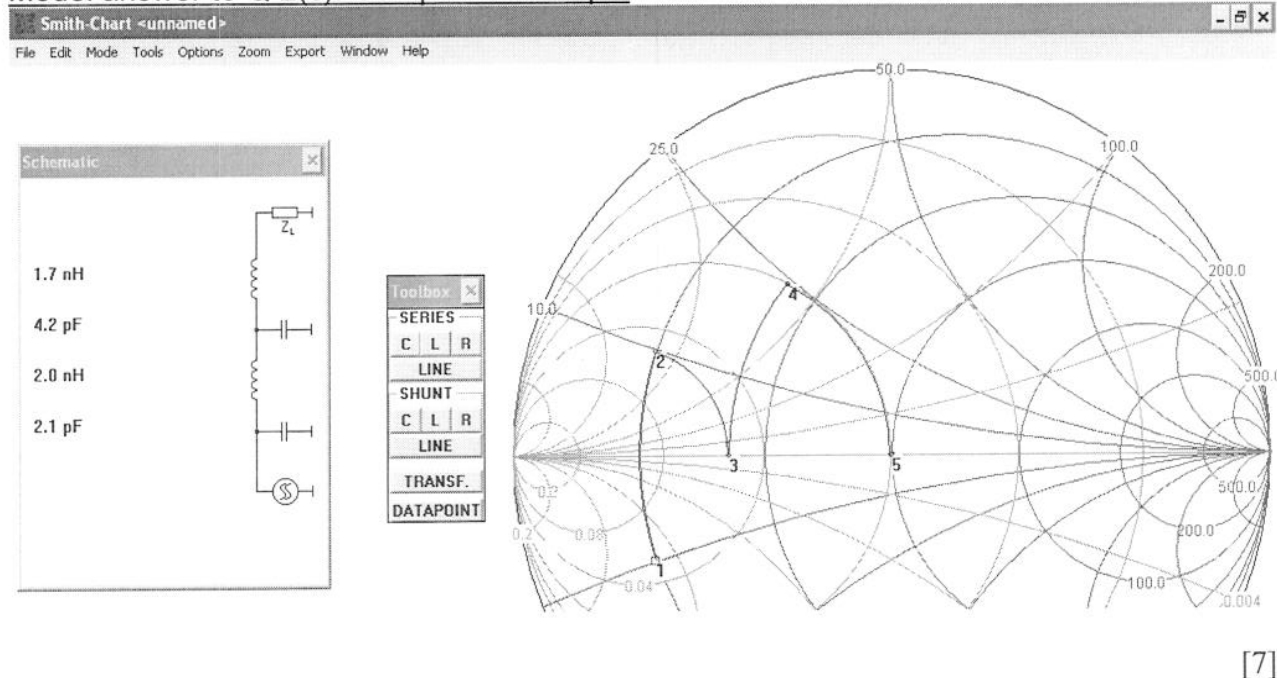
[7]



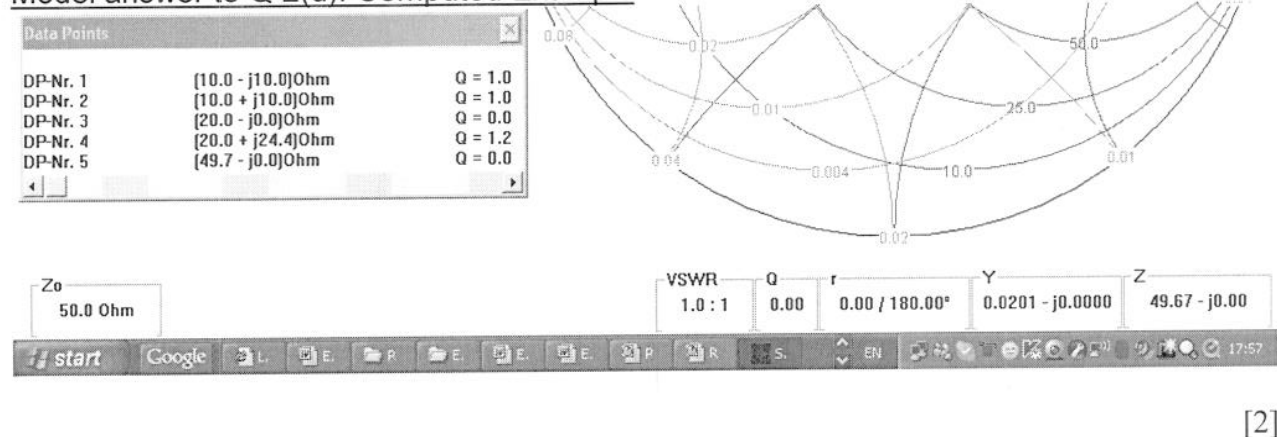
### Model answer to Q 2(b): Computed Example



### Model answer to Q 2(c): Computed Example



### Model answer to Q 2(d): Computed Example



### Model answer to Q 2(e): Bookwork

The maximum value of unloaded Q-factor in 1(b) is 1.0, while that in 1(d) is 1.2. This means that the lumped-element design has a higher than that for the distributed-element design. As a result, the operational bandwidth of the lumped-element design will be slightly narrower.

**Model answer to Q 3(a): New application of theory**

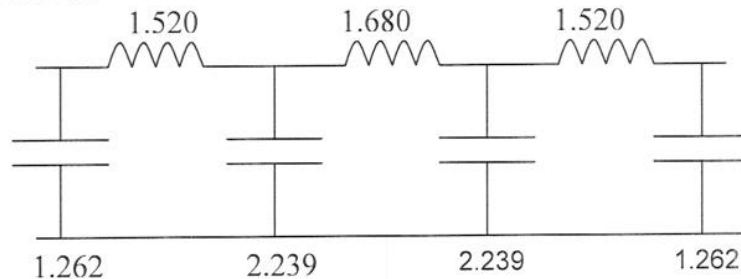
Given a square wave signal generator, with a clock frequency that can vary between zero and 1000 MHz, set the output to 600 MHz. Using a band-pass filter having a centre-frequency set to the third harmonic of the signal generator, the desired 1800 MHz sinusoidal signal can be extracted. Alternatively, a high-pass filter can be used, however, the 5<sup>th</sup> and 7<sup>th</sup> etc., harmonics will also be present but at much lower power levels.

[4]

**Model answer to Q 3(b): Bookwork and Computed Example**

From graphs provided, for Chebyshev filters with a 0.1 dB ripple, a 7<sup>th</sup> order filter is required to achieve an out-of-band rejection of > 70 dB with an  $f_c/f$  ratio of  $1500/600 = 2.5$ .

From tables provided, with  $R_S = R_L = Z_0 = 50$ , the prototype low-pass filter and associated coefficients are given below:

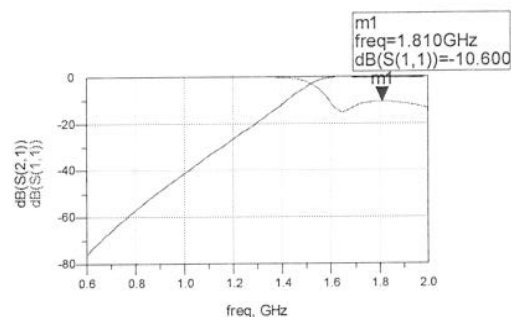
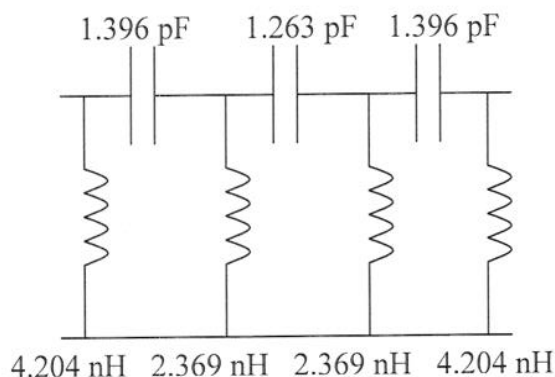
**High-pass de-normalising:**

Shunt inductor:

Series Capacitor:

$$L_p = \frac{R_L}{2\pi f_c L_n}$$

$$C_s = \frac{1}{2\pi f_c C_n R_L}$$



The slight deviation in the results from those predicted by theory are due to limited component tolerances used within the simulations.

[10]

**Model answer to Q 3(c): New application of theory**

The worst-case level of return loss within the pass band is  $10 \log[1 - \text{antilog}(-0.1/10)] = -16.43$  dB. This will have no effect within the pass band. However, well-below the pass band the return loss will be 0 dB. At the fundamental frequency of 600 MHz, all the signal will be reflected back by the filter and the square wave signal generator may not work properly (if at all). One possible solution is to insert a circulator between the square-wave generator and the filter, however, passive circulators tend to be narrow band in nature. However, a more practical solution is to use a balance topology for the filters, whereby two identical filters are embedded between two identical ultra-broadband 3 dB quadrature directional couplers. This approach is inherently impedance matched across the bandwidth of the couplers.

[6]

**Model answer to Q 4(a): Bookwork**

Devices and networks are traditionally characterised using  $Z$ ,  $Y$  or  $h$ -parameters. In order to measure these parameters directly, ideal open and short circuit terminations are required. These impedances can be easily realised at low frequencies. However, at microwave frequencies such impedances can only be achieved over narrow bandwidths (when tuned circuits are employed) and can also result in circuits that are conditionally stable (when embedded within a ‘matched load’ reference impedance environment) becoming unstable. Fortunately, scattering- (or  $S$ -) parameters can be determined at any frequency. To perform such measurements, the device under test (DUT) is terminated with matched loads. This enables extremely wideband measurements to be made and also greatly reduces the risk of instability; but only when the DUT is terminated with near ideal matched loads (this is irrespective of whether the measurement system is calibrated or not).  $S$ -parameter measurements also offer the following advantages:

1. any movement in a measurement reference plane along an ideal transmission line will vary the phase angle only (*c.f.* the complicated impedance transformation found with  $z$ -parameters)
2. for a linear device or network, voltage or current and measured power are related through the measurement reference impedance (normally 75 or 50  $\Omega$  for coaxial lines and 1  $\Omega$  for rectangular waveguides)
3. with some passive and reciprocal structures, ideal  $S$ -parameters can be deduced from spatial considerations, enabling the measurements of the structure to be checked intuitively.

While measurements are easier to perform using  $S$ -parameters, commercial RF simulators use  $Z$ - and  $Y$ -parameters to undertake the matrix calculations and then convert the results into  $S$ -parameters.

[5]

**Model answer to Q 4(b): Bookwork**

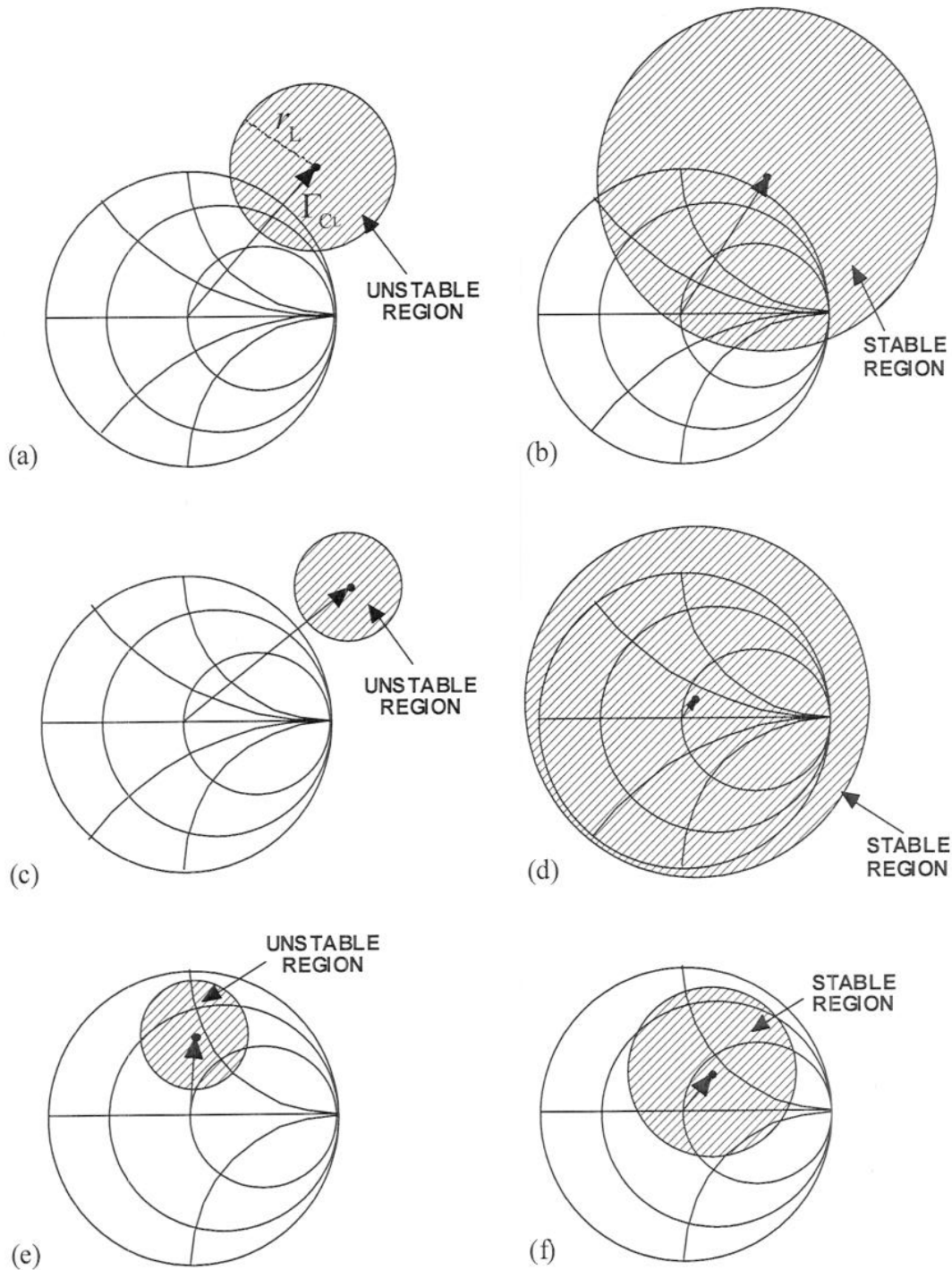
The “stability circle” represents a region on the Smith chart’s  $\rho_L$ -plane, inside (if it does not encompass the  $Z_0$  point) or outside (if it encompasses the  $Z_0$  point) of which all load impedances will make the circuit’s input reflection coefficient greater than unity, resulting in instability. The figure below shows the possible cases graphically. Regions (a), (b), (e) and (f) show conditionally stable regions, while (c) and (d) are unconditionally stable regions, for passive loads lying within the unit Smith chart.

It is very important for the designer to know straight away whether the transistor is unconditionally stable or not. Rollett’s stability factor,  $K$ , gives an immediate indication of stability and this is given by:

$$K = \frac{1 - |S_{11}|^2 - |S_{22}|^2 + |\Delta|^2}{2|S_{12}S_{21}|} \quad \text{and} \quad \Delta = S_{11}S_{22} - S_{12}S_{21}$$

If  $K > 1$  then the transistor is unconditionally stable, and if  $K < 1$  the stability depends on the position of the source and load impedances relative to the stability circles.





**Stability circles on the Smith chart: (a) stability circle partially inside the Smith chart, (b) partially inside and encompassing the  $Z_o$  point, (c) completely outside, (d) completely encompassing the Smith chart, (e) completely inside but not encompassing the  $Z_o$  point and (f) completely inside and encompassing the  $Z_o$  point**

[5]

**Model answer to Q 4(c): Bookwork**

Given the following power levels, it is possible to define Power Gain in specific ways:

$P_{AS}$  = Power Available from the Source to the Network

$P_{DN}$  = Power Delivered to the Network

$P_{AN}$  = Power Available from the Network to the Load

$P_{DL}$  = Power Delivered to the Load

‘Power Available’ simply means the absolute maximum power that can be supplied (i.e. under complex conjugate matching). ‘Power Delivered’ simply means the actual power that is dissipated.

**Insertion Power Gain**

$$G_I = \frac{P_{DL}(DUT)}{P_{DL}(no\ DUT)}$$

In practice  $G_I$  is not very meaningful since a given level can be obtained with an infinite number of  $\rho_S$  or  $\rho_L$  values.

**Forward Transducer Power Gain**

$$G_{FT} = \frac{P_{DL}}{P_{AS}}$$

This is the most useful definition for characterising the advantage of employing an amplifier, as it gives the power gain relative to an ideal matching network that would perfectly match the load impedance to the source impedance.

**Operating Power Gain**

This represents  $G_{FT}$  when the input stage is matched.

$$G_{OP} = \frac{P_{DL}}{P_{DN}}$$

This definition is independent of  $\rho_S$ . In practice,  $G_{OP}$  is useful for power amplifier designs, since the output power of the amplifier depends on the output RF load line impedance.

**Available Power Gain**

This represents  $G_{FT}$  when the output stage is matched.

$$G_{AV} = \frac{P_{AN}}{P_{AS}}$$

This definition is independent of  $\rho_L$ . In practice,  $G_{AV}$  is useful for low noise amplifier designs, since the noise figure of the amplifier depends on  $\rho_S$ .

[5]

**Model answer to Q 4(d): Bookwork and Computed Example**

When the  $K$ -factor is less than unity, the device is conditionally stable and the point of maximum gain will be inside the unstable region. In this case we have to accept that the maximum transducer gain is not achievable due to instability. Therefore, the maximum gain that can be safely achieved is called the maximum stable gain (MSG) and is given by:

$$\text{MSG} = \left| \frac{S_{21}}{S_{12}} \right| = 33.48 = 15.25 \text{ dB}$$

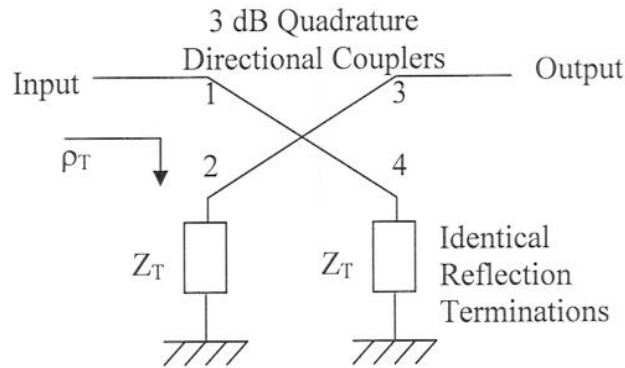
When  $K$  is greater than unity (and the magnitudes of  $S_{11}$  and  $S_{22}$  are both less than unity), the device is unconditionally stable and the maximum gain that can be achieved is called the maximum available gain (MAG), given by:

$$\text{MAG} = \left| \frac{S_{21}}{S_{12}} \right| \left( K - \sqrt{K^2 - 1} \right) = 33.48 \times 0.487 = 16.31 = 12.12 \text{ dB}$$

Typically, a transistor is conditionally stable ( $K < 1$ ) at low frequencies, and the maximum stable gain rolls off at 3 dB per octave. At a certain frequency  $K = 1$ , and beyond that the device is unconditionally stable ( $K > 1$ ) and the maximum available gain rolls off at 6 dB per octave.

[5]

#### Model answer to Q 5(a): New Derivation



$$S_{21} |_{\text{OVERALL}} = S_{21} \rho_T S_{41} + S_{41} \rho_T S_{21} = 2 S_{21} \rho_T S_{41}$$

For a 3 dB quadrature coupler:

$$S_{41} = \frac{1}{\sqrt{2}} e^{-j\frac{\pi}{2}} \quad \text{and} \quad S_{21} = \frac{1}{\sqrt{2}} e^{-j0}$$

$$\therefore S_{21} |_{\text{OVERALL}} = 2 \frac{1}{\sqrt{2}} e^{-j\frac{\pi}{2}} \rho_T \frac{1}{\sqrt{2}} = \rho_T e^{-j\frac{\pi}{2}}$$

The reflection topology transforms a reflection coefficient into a transmission coefficient.

[7]

#### Model answer to Q 5(b) New Derivation

Here the reflection coefficient is implemented with a PIN diode or cold-FET, to realise a variable resistance,  $R_T$ .

$$\rho_T(V) = \frac{R_T(V) - Z_0}{R_T(V) + Z_0} \equiv |\rho_T(V)|$$

$$\therefore S_{21} |_{\text{OVERALL}} = |\rho_T(V)| e^{-j\frac{\pi}{2}}$$

Therefore, the relative attenuation,  $\Delta |S_{21}|_{\text{OVERALL}} = \Delta |\rho_T(V)|$

[5]

#### Model answer to Q 5(c) New Derivation

Here the reflection coefficient is implemented with a varactor diode, to realise a variable

capacitance,  $C_T = \frac{-1}{\omega X_T}$ .

$$\rho_T(V) = \frac{X_T(V) - Z_0}{X_T(V) + Z_0} \equiv 1.e^{j\angle\rho_T(V)}$$

$$\therefore S_{21}|_{\text{OVERALL}} = 1.e^{j\angle\rho_T(V) - j\frac{\pi}{2}}$$

Therefore, the relative phase shift,  $\Delta\angle S_{21}|_{\text{OVERALL}} = \Delta\angle\rho_T(V)$

[5]

#### Model answer to Q 5(d) Extended Textbook

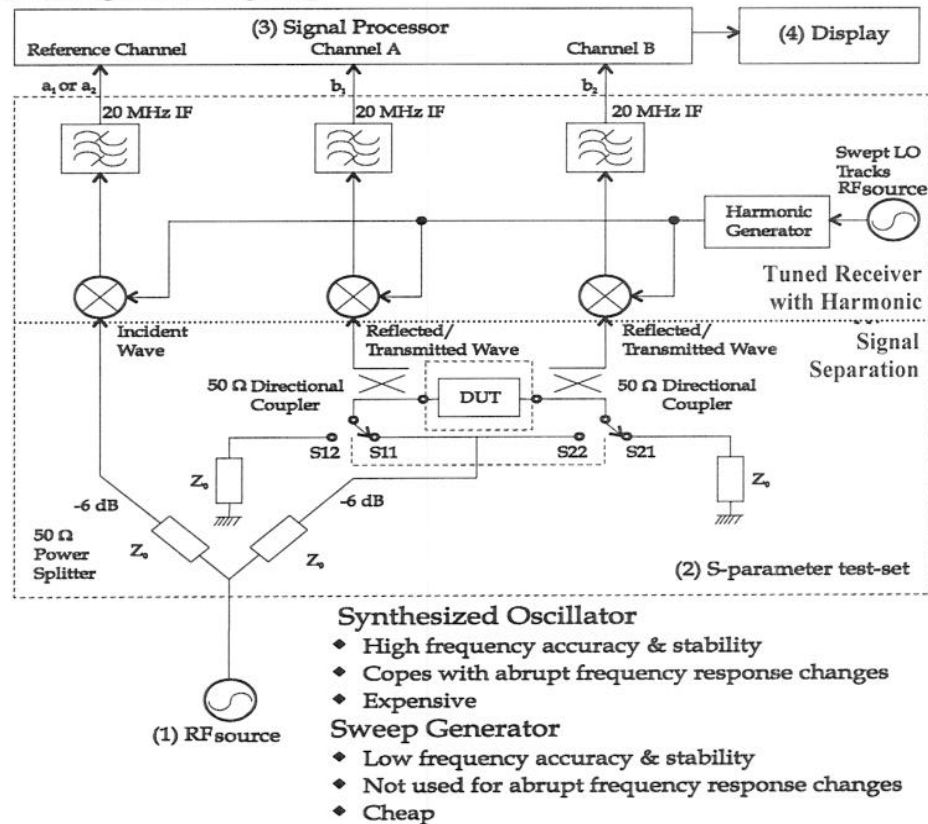
The attenuation suffers from AM-PM conversion, due to parasitic reactive elements. The phase shifter suffers from PM-AM conversion due to parasitic resistive elements. A useful vector modulator can be implemented by simply cascading a reflection-type attenuator with a reflection-type phase shifter.

[3]

#### Model answer to Q6(a): Bookwork

A cheap scalar network analyser consists of an RF<sub>SOURCE</sub>, a 2-resistor power splitter (which has excellent frequency response across an ultra-wide bandwidth), a wideband diode detector (at low RF power it has a square-law response, i.e. the output DC voltage is proportional to the absorbed RF power; this response then goes linear at higher RF power levels) and processor/display. *[The student can draw this]*. Apart from delivering fast measurements, a very useful application of the scalar network analyser is its ability to characterise the transmission properties of mixers, where the incident signal will be at a different frequency to the output signal. Only the magnitude of transmission measurements are possible. Here, the source and detector are connected together and then the device under test is inserted. The difference in measurements gives the insertion loss.

The equipment most commonly used is called a vector network analyser (VNA), because this instrument can also measure the phase angle of the S-parameters. As a result, the DUT can now be characterised using complete S-parameter measurements (along with DC measurements). Compared to direct diode detection, tuned receivers have a higher dynamic range, are immune from harmonic and spurious responses, can measure phase and, therefore, facilitate better calibration techniques. Amplitude measurements are taken from the relative ratio of an unknown signal (test channel A or B) to a reference signal (reference channel). Phase measurements are taken from the relative phase difference between the test and reference channels. *[The student only needs to have the outline of the following block diagram].*



[8]

Model answer to Q6(b): Bookwork

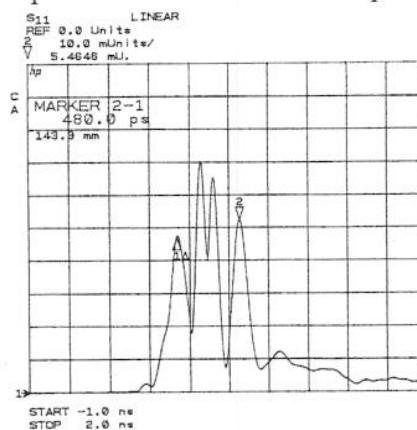
When compared with test fixtures, commercial probe station measurements:

- (1) Are available in a single-sweep system from DC to 120 GHz, whereas commercial test fixtures can operate from DC to 60 GHz.
- (2) Are more accurate and much more repeatable, since they introduce much smaller systematic errors.
- (3) Have a simpler calibration procedure, which can be automated with on-wafer calibration and verification standards.
- (4) Enable the VNA measurement reference planes to be located at the probe tips or at some distance along the MMIC's transmission line. In the latter case, transition effects can be removed all together.
- (5) Provide a fast, non-destructive means of testing the MMIC, thus allowing chip selection prior to dicing and packaging.
- (6) Overall, the microwave probe station can provide the most cost effective way of measuring MMICs when all costs are taken into account.

[4]

Model answer to Q6(c): Bookwork

Some VNAs can perform synthetic-pulse time-domain reflectometry (TDR). Here, the discrete form of the inverse Fourier transform (IFT) is applied to a real sequence of harmonically related frequency-domain (F-D) measurements. This is directly equivalent to mathematically generating synthetic unity-amplitude impulses (or unity-amplitude steps), which are then 'applied' to the embedded DUT. The resulting time-domain (T-D) reflection and transmission responses can then be analysed to provide information about the DUT and test fixture discontinuities. In reflection measurements, it is possible to remove the effects of unwanted impedance mismatches or else isolate & view the response of an individual feature. With a multiple port test-fixture, transmission measurements can give the propagation delay & insertion loss of signals travelling through a particular path by removing the responses from the unwanted paths.



### Time-domain response for the input voltage reflection coefficient of an embedded mismatched MMIC through-line

The frequency response of  $|S_{11}|$  can be emphasised for the embedded MMIC by gating out the two outer peaks in the associated time-domain response. This 'de-embedding' process is not needed with on-wafer probing, as the reference planes are located at the probe tips. In other words, any connectors have already been calibrated out.

[8]